2014 IEEE International Conference on Robotics & Automation (ICRA)
Hong Kong Convention and Exhibition Center
May 31 - June 7, 2014. Hong Kong, China

Dynamics Modeling and Identification of the Human-Robot Interface Based on a Lower Limb Rehabilitation Robot

Weiqun Wang, Zeng-Guang Hou, Lina Tong, Yixiong Chen, Liang Peng, and Min Tan

***Abstract*— A lower limb rehabilitation robot, namely *iLeg*, has been developed recently. Since active exercises have been proven to be effective for neurorehabilitation and motor recovery, they are suggested to be implemented on *iLeg*. To this goal, patients' motion intention should be recognized. Therefore, a method based on the dynamic model of the human-robot interface (HRI) is designed to recognize the human motion intention. This paper is devoted to modeling and identifying the dynamics of the HRI. Firstly, the dynamic model of the HRI is designed by combining the dynamic models of the human leg and *iLeg*, where the human leg dynamic model (HLDM) is mainly concerned. By considering the motion trajectories during the rehabilitation exercises provided by *iLeg*, the human leg can be taken as a manipulator with two degrees of freedom; meanwhile, the joint angles and torques of the human leg can be measured indirectly by using the position and torque sensors mounted on the joints of *iLeg*. As a result, an 8-parameter HLDM can be designed by using the Lagrangian method. Then, the dynamic model of the HRI is identified by respectively and independently identifying the undetermined dynamic parameters of *iLeg* and the HLDM, where the dynamic parameters of the HLDM are mainly considered. Finally, the feasibility of the dynamic model of the HRI is validated by experiments.**

I. Introduction

The number of patients with lower limb dysfunctions including paraplegia and hemiplegia is increasing rapidly in recent years because of various causes, especially stroke [1] and spinal cord injury (SCI) [2] brought out by traffic accidents or natural calamities. It usually needs long time to recover from the suffering for the patients after the instant therapy. The traditional methods for lower limb rehabilitation usually need lots of physicians and nurses, and hence, impose heavy social and economic burden on the family and society. Therefore, more and more attentions have been paid to lower limb rehabilitation robot (LLRR), which is supposed to be able to provide personal rehabilitation prescriptions, enhance the effects, and meanwhile reduce the burden of the associated people. Recently, an LLRR prototype, namely *iLeg*, has been developed at Institute of Automation, Chinese Academy of Sciences. As shown in Fig. 1, *iLeg* consists of three parts: one chair and two leg mechanisms. Both the leg mechanisms, with the same structures, have three degrees of freedom (DOFs): the hip, knee, and ankle joints. In this paper, one of the leg mechanisms is referred as *iLeg* for easy description.

*The authors are with State Key Laboratory of Management and Control for Complex Systems, Institute of Automation, Chinese Academy of Sciences, Beijing 100190, China (weiqun.wang@ia.ac.cn, hou@compsys.ia.ac.cn.)

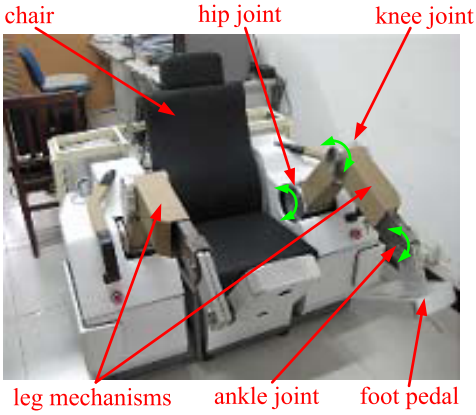

Fig. 1. The prototype of *iLeg*.

A. Recognition of the Human Motion Intention

According to whether or not the voluntary intention of the patients is involved, rehabilitation exercises can basically be divided into two kinds: passive and active exercises. Although the passive exercises, in which the voluntary intention is not involved, can be implemented more easily by rehabilitation robots or machines, the active ones are more effective for neurorehabilitation and motor recovery [3], and hence have received more attentions nowadays. In order to implement active rehabilitation exercises, the voluntary motion intention of the patients should be recognized, which in the literature has been carried out by using the electromyography (EMG) [4] or electroencephalogram (EEG) [5] signals. Whereas, it is shown in the clinical trials that EMG and EEG signals have a strong dependence on individuals and a plenty of factors can affect the accuracy of the estimation. Therefore, it is difficult and complicated to use EMG and EEG signals in rehabilitation practice.

In this paper, position and torque sensors are used to recognize the human motion intention, since the information from these sensors is more reliable and robust. The proposed active rehabilitation exercise architecture is given in Fig. 2, where the torques and joint angles are measured by the associated sensors which are mounted on both the hip and knee joints of *iLeg*.

It can be seen from Fig. 2 that the human motion intention is recognized based on the dynamic model of the human-robot interface (HRI) of *iLeg*. The HRI dynamics consists of two components: the dynamics of the human leg and *iLeg*. Therefore, the dynamic model of the HRI is derived in this way: firstly, the dynamics of the human leg and *iLeg* are

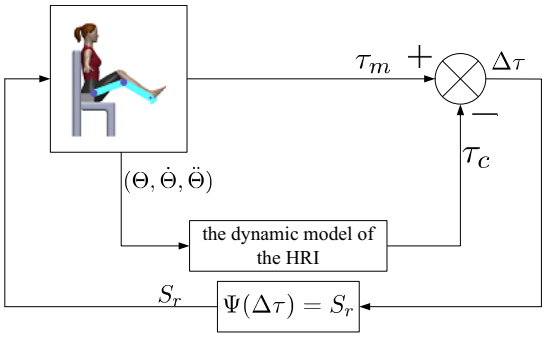

Fig. 2. The active rehabilitation exercise architecture based on the dynamic model of the human-robot interface (HRI). $\boldsymbol{\tau_m}$ and $\boldsymbol{\tau_c}$ are respectively the measured and estimated torque vectors, where $\boldsymbol{\tau_c}$ is calculated from the dynamic model of the HRI. $\boldsymbol{S_r}$, the velocity or position vector depending on the control strategy, is derived from $\boldsymbol{\Delta\tau}$ which represents the human motion intention.

identified respectively and independently, and then the HRI dynamics is obtained by combining the two components. In this paper, the human leg dynamic model (HLDM) is mainly concerned; meanwhile, the dynamic model of *iLeg* is designed by using the traditional method.

B. Dynamics of the Human Leg

Usually human dynamic model is designed to be suitable for a particular type of motions and the specific circumstance. In [6], a simple 3-segment human body model was designed in order to reconstruct the motion trajectories of the shank, thigh and head-arms-trunk (HAT) segments in sit-to-stand motion by using low-cost inertial sensors. A 54 DOFs model suitable for analysis of skilled motions such as movements in sports, driving movements, etc., was proposed in [7], where the HLDM had 14 DOFs for each leg. The most commonly used human dynamic model is a 15 links model with 34 DOFs, where the HLDM has 7 DOFs: both the hip and ankle joints are taken as spherical joints and have 3 DOFs, respectively; the knee joint has 1 DOF [8]. It has been proven in [7], more complex models can describe more precisely the kinematics of human motions. Whereas, the computational load will increase and the stability will decrease when the complexity of the models rises. Therefore, it is usually a trade-off among the estimation precision, stability, and computational load.

When patients are doing rehabilitation exercises with *iLeg*, motions of their legs are restricted in the sagittal plane; hence, the hip and ankle joints have only 1 DOF respectively. Moreover, in the exercises provided by *iLeg*, the angular range of the ankle joint is relatively small and has little effect on the dynamics, therefore the ankle joint is neglected in the HLDM of this paper. As a result, the lower limb of the patient doing rehabilitation exercise with *iLeg* can be regarded as a 2 DOFs planar manipulator.

In order to implement parameters estimation of the HLDM, joint torques or contact forces between the human foot and the pedal or other foot supporter, which can be converted to joint torques by the Jacobian matrix, should be measured. In [9], the contact force measured by the force-plate was

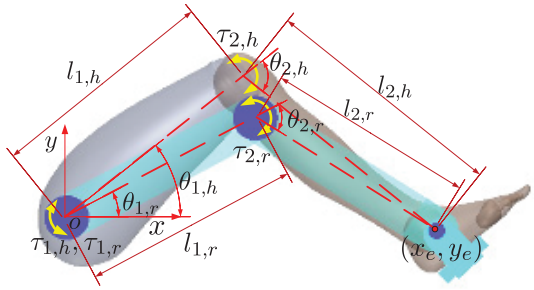

Fig. 3. The schematic plot of the HRI. The hip and ankle joints axes of the human leg match those of *iLeg* well. The knee joint axis of the human leg usually does not match that of *iLeg* since lengths of the thigh and crus of the human leg usually don't exactly equal to the corresponding links of *iLeg*.

used to identify the inertial parameters since joint torques of the human leg are usually more difficult to be measured in practice. Whereas, as for *iLeg*, torques measured by the torque sensors mounted on the joints are more robust to the disturbance on the foot pedal, which is common in the rehabilitation exercises. Furthermore, the method using force sensors mounted on the foot pedal to recognize the patients' motion intention will impose additional constraints on the patients' feet, which will inevitably lead to uncomfortable manipulations. Therefore, in this paper, the torque and position sensors mounted on both the hip and knee joints of *iLeg* are used to identify the HLDM and to recognize the human motion intention.

The remainder of this paper is organized as follows: Section II describes the dynamic model of the HRI and the identification method; the experiments and results are given in Section III; the paper is concluded in Section IV.

II. Modeling and Identification of the HRI Dynamics

The schematic plot of the HRI based on *iLeg* is given in Fig. 3. It is shown that, the HRI consists of two components: the human leg and *iLeg*, where the hip and ankle joints of the human leg respectively well match those of *iLeg*. As analyzed in the above section, both ankle joints of the two components are neglected, such that both the human leg and *iLeg* have two 2 DOFs and can be taken as 2 DOFs robots, respectively. The dynamic model of the HRI is derived by combining the HLDM and the dynamic model of *iLeg*.

A. The HLDM

Since the human leg doing exercises with *iLeg* can be taken as a 2 DOFs robot, the methods for modeling robotic dynamics can be used to design the HLDM. In this paper, the Lagrangian equations are used, which are defined by:

$$\tau_{i,h} = \frac{d}{dt}\left(\frac{\partial L_h}{\partial \dot{\theta}_{i,h}}\right) - \frac{\partial L_h}{\partial \theta_{i,h}}, \forall i = 1, 2, \tag{1}$$

where $\tau_{i,h}$, $\theta_{i,h}$, and $\dot{\theta}_{i,h}$ are respectively the ith joint torque, angle, and angular velocity of the human leg, as is shown in Fig. 3; L_h, the Lagrangian function of the system, is defined

by:

$$L_h = K_h(\mathbf{\Theta}_h, \dot{\mathbf{\Theta}}_h) - P_h(\mathbf{\Theta}_h), \tag{2}$$

where K_h and P_h are respectively the kinetic and potential energies; $\mathbf{\Theta}_h = (\theta_{1,h}, \theta_{2,h})^T$ and $\dot{\mathbf{\Theta}}_h = (\dot{\theta}_{1,h}, \dot{\theta}_{2,h})^T$ are respectively the angle and angular velocity vectors.

In order to model the dynamics of the human leg as accurately as possible, the integral method is used to derive the kinetic and potential energies. The joint friction model is derived from the traditional friction model of robotic manipulator given in [10] by neglecting the Coulomb friction. Then, by eliminating the similar terms and regrouping the parameters, the following HLDM can be obtained:

$$\mathbf{\Phi}_h(\mathbf{\Theta}_h, \dot{\mathbf{\Theta}}_h, \ddot{\mathbf{\Theta}}_h)\mathbf{P}_h = \boldsymbol{\tau}_h, \tag{3}$$

where $\mathbf{\Phi}_h$ is a 2×8 function matrix, representing the regressor; $\boldsymbol{\tau}_h = [\tau_{1,h}, \tau_{2,h}]^T$, is the torque vector in the human leg joint space; $\mathbf{P}_h$ is the dynamic parameter vector. The elements of $\mathbf{\Phi}_h$ and $\mathbf{P}_h$ are defined respectively by:

$$\begin{aligned}
&\phi^h_{1,1} = 2\ddot{\theta}_{1,h}, \quad \phi^h_{1,2} = \cos(\theta_{1,h}),\\
&\phi^h_{1,3} = 2\ddot{\theta}_{1,h} + 2\ddot{\theta}_{2,h},\\
&\phi^h_{1,4} = 2\ddot{\theta}_{1,h}\cos(\theta_{2,h}) + \ddot{\theta}_{2,h}\cos(\theta_{2,h})\\
&\qquad - 2\dot{\theta}_{1,h}\dot{\theta}_{2,h}\sin(\theta_{2,h}) - \dot{\theta}^2_{2,h}\sin(\theta_{2,h})\\
&\qquad + g\cos(\theta_{1,h} + \theta_{2,h})/l_{1,h},\\
&\phi^h_{1,5} = -2\dot{\theta}_{1,h}\dot{\theta}_{2,h}\cos(\theta_{2,h}) - \dot{\theta}^2_{2,h}\cos(\theta_{2,h})\\
&\qquad - 2\ddot{\theta}_{1,h}\sin(\theta_{2,h}) - \ddot{\theta}_{2,h}\sin(\theta_{2,h})\\
&\qquad - g\sin(\theta_{1,h} + \theta_{2,h})/l_{1,h},\\
&\phi^h_{1,6} = -\sin(\theta_{1,h}), \quad \phi^h_{1,7} = \dot{\theta}_{1,h}, \quad \phi^h_{1,8} = 0,\\
&\phi^h_{2,1} = 0, \quad \phi^h_{2,2} = 0, \quad \phi^h_{2,3} = 2\ddot{\theta}_{1,h} + 2\ddot{\theta}_{2,h},\\
&\phi^h_{2,4} = \dot{\theta}^2_{1,h}\sin(\theta_{2,h}) + \ddot{\theta}_{1,h}\cos(\theta_{2,h})\\
&\qquad + g\cos(\theta_{1,h} + \theta_{2,h})/l_{1,h},\\
&\phi^h_{2,5} = \dot{\theta}^2_{1,h}\cos(\theta_{2,h}) - \ddot{\theta}_{1,h}\sin(\theta_{2,h})\\
&\qquad - g\sin(\theta_{1,h} + \theta_{2,h})/l_{1,h},\\
&\phi^h_{2,6} = 0, \quad \phi^h_{2,7} = 0, \quad \phi^h_{2,8} = \dot{\theta}_{2,h},
\end{aligned} \tag{4}$$

and

$$\begin{aligned}
p^h_1 &= \int_{V_1} \frac{1}{2}\rho_v l_v^2 dv + \int_{V_2} \frac{1}{2}\rho_v l^2_{1,h} dv,\\
p^h_2 &= \int_{V_1} \rho_v l_v g\cos(\theta_v) dv + \int_{V_2} \rho_v l_{1,h} g dv,\\
p^h_3 &= \int_{V_2} \frac{1}{2}\rho_v l_v^2 dv, \quad p^h_4 = \int_{V_2} \rho_v l_v \cos(\theta_v) l_{1,h} dv,\\
p^h_5 &= \int_{V_2} \rho_v l_v \sin(\theta_v) l_{1,h} dv,\\
p^h_6 &= \int_{V_1} \rho_v g l_v \sin(\theta_v) dv, \quad p^h_7 = c_{1,1}, \quad p^h_8 = c_{2,1},
\end{aligned} \tag{5}$$

where V_1 and V_2 are respectively the volumes of the human thigh and crus; dv is a micro-element. ρ_v, l_v and θ_v, all correlated with the location, are respectively the material density, the distance between dv and the associated joint axis, and the angular deviation of dv from the center line; g is the gravitational acceleration; $c_{1,1}$ and $c_{2,1}$ respectively describe the damping characteristics of the hip and knee joints; p^h_1 - p^h_8 are the undetermined parameters to be identified.

B. The Dynamic Model of iLeg

The dynamic model of *iLeg* used in this paper is derived by using the traditional joint friction model given in [10] and the Lagrangian method. The obtained dynamic model is given by:

$$\mathbf{\Phi}_r(\mathbf{\Theta}_r, \dot{\mathbf{\Theta}}_r, \ddot{\mathbf{\Theta}}_r)\mathbf{P}_r = \boldsymbol{\tau}_r, \tag{6}$$

where $\mathbf{\Phi}_r$ is a 2×12 regressor matrix and all of the elements of $\mathbf{\Phi}_r$ are functions of the joint angles, angular velocities and accelerations of *iLeg*, which are represented by $\mathbf{\Theta}_r$, $\dot{\mathbf{\Theta}}_r$ and $\ddot{\mathbf{\Theta}}_r$, respectively; $\mathbf{P}_r$, a 12×1 vector, represents the dynamic parameters for *iLeg*; $\mathbf{\Theta}_r = [\theta_{1,r}, \theta_{2,r}]^T$; $\boldsymbol{\tau}_r = [\tau_{1,r}, \tau_{2,r}]^T$.

C. The Dynamic Model of the HRI

By combining the HLDM and the dynamics of *iLeg*, the following dynamic model of the HRI can be obtained:

$$\boldsymbol{J}_r^T \boldsymbol{J}_h^{-T} \mathbf{\Phi}_h(\mathbf{\Theta}_h, \dot{\mathbf{\Theta}}_h, \ddot{\mathbf{\Theta}}_h)\mathbf{P}_h + \mathbf{\Phi}_r(\mathbf{\Theta}_r, \dot{\mathbf{\Theta}}_r, \ddot{\mathbf{\Theta}}_r)\mathbf{P}_r = \boldsymbol{\tau}_{hri}, \tag{7}$$

where the first term represents the contribution of the HLDM, which is derived by mapping the joint torques in the joint space of the human leg into that of *iLeg*; $\boldsymbol{\tau}_{hri}$ is the total joint toque vector of the HRI, which can be measured by the torque sensors mounted on *iLeg* joints; $\boldsymbol{J}_h$ and $\boldsymbol{J}_r$ are Jacobian matrixes respectively for the human leg and *iLeg*, which are defined respectively by:

$$\boldsymbol{J}_h = \begin{bmatrix} J^h_{1,1} & J^h_{1,2} \\ J^h_{2,1} & J^h_{2,2} \end{bmatrix}, \quad \boldsymbol{J}_r = \begin{bmatrix} J^r_{1,1} & J^r_{1,2} \\ J^r_{2,1} & J^r_{2,2} \end{bmatrix}, \tag{8}$$

where

$$\begin{aligned}
J^h_{1,1} &= -l_{1,h}\sin(\theta_{1,h}) - l_{2,h}\sin(\theta_{1,h} + \theta_{2,h}),\\
J^h_{1,2} &= -l_{2,h}\sin(\theta_{1,h} + \theta_{2,h}),\\
J^h_{2,1} &= l_{1,h}\cos(\theta_{1,h}) + l_{2,h}\cos(\theta_{1,h} + \theta_{2,h}),\\
J^h_{2,2} &= l_{2,h}\cos(\theta_{1,h} + \theta_{2,h}),\\
J^r_{1,1} &= -l_{1,r}\sin(\theta_{1,r}) - l_{2,r}\sin(\theta_{1,r} + \theta_{2,r}),\\
J^r_{1,2} &= -l_{2,r}\sin(\theta_{1,r} + \theta_{2,r}),\\
J^r_{2,1} &= l_{1,r}\cos(\theta_{1,r}) + l_{2,r}\cos(\theta_{1,r} + \theta_{2,r}),\\
J^r_{2,2} &= l_{2,r}\cos(\theta_{1,r} + \theta_{2,r}).
\end{aligned}$$

D. Identification of the Dynamic Model of the HRI

It is shown by (7), both components of the dynamic model of the HRI are linear, and hence can be identified by the traditional identification method. Since the joint angles and torques of *iLeg* can be measured directly by the associated sensors, the dynamic model of *iLeg* is identified first. Then, the HLDM defined by (3) is identified, where the joint angles and torques of the human leg should be obtained before the parameter estimation.

The joint angles of the human leg can be derived from

those of *iLeg* as follows:

$$\theta_{2,h} = \arccos\left(\frac{l_{1,r}^2 + l_{2,r}^2 + 2l_{1,r}l_{2,r}\cos(\theta_{2,r}) - l_{1,h}^2 - l_{2,h}^2}{2l_{1,h}l_{2,h}}\right),$$
$$\theta_{1,h} = \begin{cases} -\arctan(b/a) + \arcsin(c), & if\ a > 0 \\ \pi - \arctan(b/a) + \arcsin(c), & if\ a \le 0 \end{cases}, \tag{9}$$

where

$$a = l_{1,h} + l_{2,h}\cos(\theta_{2,h}),$$
$$b = l_{2,h}\sin(\theta_{2,h}),$$
$$c = \frac{l_{1,r}\sin(\theta_{1,r}) + l_{2,r}\sin(\theta_{1,r} + \theta_{2,r})}{\sqrt{l_{1,h}^2 + l_{2,h}^2 + 2l_{1,h}l_{2,h}\cos(\theta_{2,h})}}.$$

When the human leg is in the quiescent condition, the torque measured by the associated torque sensor is a combination of the torques contributed by the dynamics of the human leg and *iLeg*. Therefore, the joint torque contributed by the human leg dynamics can be obtained by the following equation:

$$\boldsymbol{\tau}_{hri}^h = \boldsymbol{\tau}_{hri}^m - \boldsymbol{\tau}_{hri}^r, \tag{10}$$

where $\boldsymbol{\tau}_{hri}^m$ is a joint torque vector which is measured at the joints of *iLeg*; $\boldsymbol{\tau}_{hri}^h$ and $\boldsymbol{\tau}_{hri}^r$ represent the joint torques contributed by the dynamics of human leg and *iLeg*, respectively; $\boldsymbol{\tau}_{hri}^r$ can be calculated by using the dynamic model of *iLeg* defined by (6). Then, $\boldsymbol{\tau}_{hri}^h$ is mapped into the joint space of the human leg by the following equation:

$$\boldsymbol{J}_h^T \boldsymbol{J}_r^{-T} \boldsymbol{\tau}_{hri}^h = \boldsymbol{\tau}_h. \tag{11}$$

Since $\boldsymbol{\Phi}_h$ and $\boldsymbol{\tau}_h$ can be obtained by (4) and (8) - (11), the undetermined parameters in (3) can be identified by using the traditional method for identifying the robotic dynamics. The exciting trajectory for identifying the HLDM is parameterized by the FFS method [11] and optimized by using the condition number criterion [12] and the particle swarm optimization (PSO) algorithm [13]. Then the designed optimal exciting trajectory (OET) is implemented on *iLeg* when the human leg is bound to it near the ankle joint and maintaining in the quiescent condition, and the torques and joint angles are measured and recorded at the same time. The obtained torques are then preprocessed by the moving average filter, which is carried out by the smooth function in the Matlab environment. The result data are mapped into the joint space of the human leg. The joint angular velocities and accelerations of the human leg can be obtained from the associated joint angles by using the numerical differential method. Finally, the undetermined parameters in (3) can be estimated by using the ordinary or weighted least square estimation (LSE) method [14].

III. Experiments and Results

The experiment setup is given in Fig. 4, where the human leg is bound on *iLeg* near the ankle joint and the human hip and ankle joints well match the corresponding joints of *iLeg*. The lengths of the human thigh and crus and those of the corresponding parts of *iLeg* are given respectively by: $l_{1,h} = 390$ mm, $l_{2,h} = 500$ mm, $l_{1,r} = 370$ mm, and $l_{2,r} = 530$ mm. Two experiments have been carried out: 1) identification of the HLDM; 2) validation of the HRI dynamic model.

Fig. 4. Experiment setup for identification and validation of the HRI dynamic model.

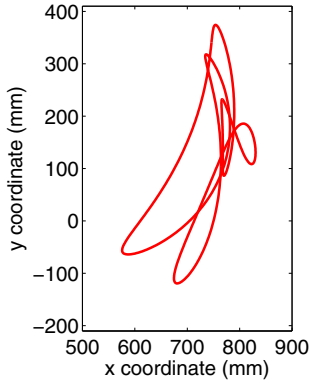

Fig. 5. The trajectory of the foot pedal for the OET.

A. Experiment for Identification of the HLDM

The OET for identifying the HLDM is given in Figs. 5 and 6. The condition number of the associated regressor matrix is 28.38, which is small enough for parameter estimation. The OET was implemented on *iLeg* repeatedly, and the hip and knee joint angles and torques were recorded at the same time. Twelve periods of data were recorded and

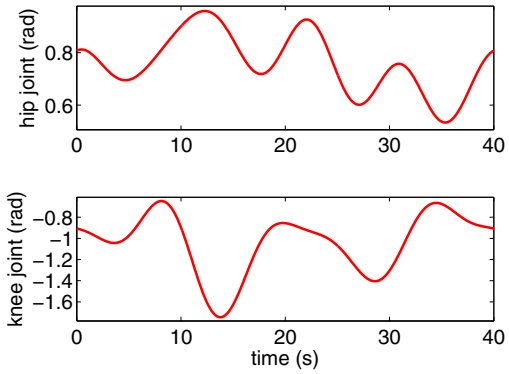

Fig. 6. The joint angles for the OET.

TABLE I

PARAMETERS ESTIMATED BY THE LSE METHOD FOR THE HLDM.

parameter	unit	value	parameter	unit	value
p_1^h	kg·m^2	0.4952	p_5^h	kg·m^2	0.1444
p_2^h	Nm	24.4210	p_6^h	Nm	11.7963
p_3^h	kg·m^2	0.6161	p_7^h	Nm·s	14.6621
p_4^h	kg·m^2	0.5140	p_8^h	Nm·s	-1.3876

the data of the first and last periods were neglected. The measured torques were preprocessed by the smooth function in the Matlab environment firstly, where the span of the function was 9. Then the torques contributed by *iLeg* were eliminated and the remainders were mapped into the joint space of the human leg; the human joint angles were obtained from the joint angles of *iLeg* and used to calculate joint velocities and accelerations subsequently by using the numerical differential method. Since the joint angles measured by using the position sensors were relatively stable and the variation was relatively small, the effect of the noise on the joint velocities was neglected. Meanwhile, the obtained accelerations were filtered by using the smooth function. Finally, the undetermined parameters of the HLDM defined by (3) were estimated by the LSE method. The results are given in Table I. The dynamic model of the HRI were obtained by combining the HLDM and the dynamic model of *iLeg*.

B. Experiment for Validation of the HRI Dynamic Model

In the validation experiment, a trajectory different from the OET, was designed and implemented on *iLeg* under the condition the same as the identification experiment. The torques and joint angles were recorded and preprocessed. Then, the joint angular velocities and accelerations were derived from the recorded joint angles and used to estimate the joint torques by using the dynamic model of the HRI identified in the above subsection. Finally, the estimated torques were compared with the torques measured by the torque sensors.

The trajectory for validation of the HRI dynamic model is given in Figs. 7 and 8. The measured and estimated torques are given in Fig. 9. The estimated torque errors are given in Table II, where τ_{rmse} is the root-mean-square error of the estimated torques defined by the following equation:

$$\tau_{rmse} = \sqrt{\frac{1}{K_c}\sum_{k=1}^{K_c}(\tau_{e,k} - \tau_{m,k})^2}, \tag{12}$$

where K_c is the number of the sampled points used in the calculation; $\tau_{e,k}$ and $\tau_{m,k}$ are respectively the kth estimated and measured torques for the hip or knee joints. β_{are} is the average relative error of the estimated joint torques, which is defined by:

$$\beta_{are} = \sqrt{\frac{1}{2K_c}\sum_{k=1}^{2K_c}\left(\frac{\tau_{e,k} - \tau_{m,k}}{\tau_{m,k}}\right)^2}, \tag{13}$$

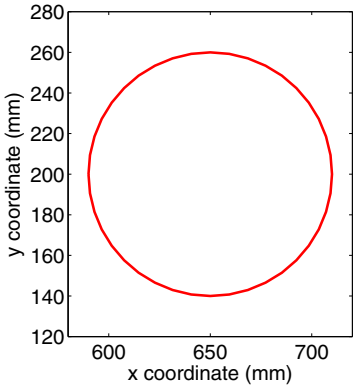

Fig. 7. The trajectory for validation of the HRI dynamic model.

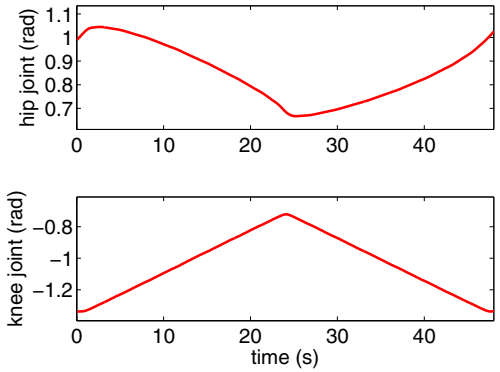

Fig. 8. The joint angles for the validation trajectory.

where β_{are} is calculated for the trajectories of the hip and knee joints together.

It can be seen that, the estimation error is small for both the hip and knee joints, which denotes that the proposed dynamic model of the HRI is suitable for torque estimation. Meanwhile, the estimation error for the hip joint is relatively big, such that further investigation needs to be carried out if a more accurate estimation is required.

IV. CONCLUSION

A method based on the joint torque estimation is proposed to recognize the human motion intention for active rehabilitation exercises, which have been proven effective for neurorehabilitation and motor recovery for the patients with lower limb dysfunctions. In order to estimate the joint torques, the dynamics of the HRI need to be identified. In this paper, the dynamic model of the HRI are divided into

TABLE II

THE ESTIMATED TORQUE ERRORS FOR THE VALIDATION TRAJECTORY.

τ_{rmse}(Nm)		
hip	knee	β_{are}
1.3288	0.3450	0.0139

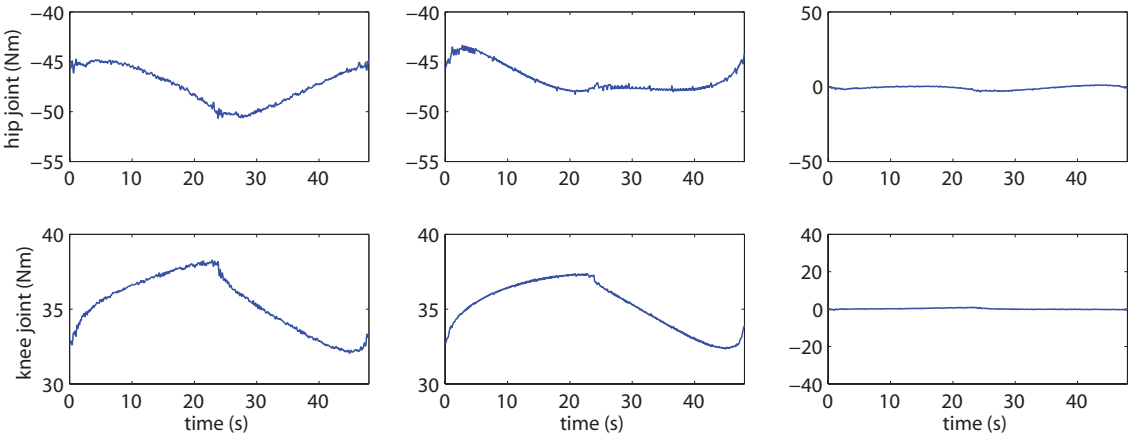

(a) (b) (c)

Fig. 9. Joint torques for the validation trajectory. (a) The measured and (b) estimated joint torques. (c) The estimated torque errors.

two components: the HLDM and the dynamic model of *iLeg*, where the HLDM is mainly concerned.

Since the motions of the human leg are restricted in the sagittal plane during the rehabilitation exercises provided by *iLeg*, and the ankle joint has little effect on the HLDM, the human leg is taken as a 2 DOFs planar robot. Therefore, the methods for modeling and identifying the dynamics of series robot can be used. An 8-parameter HLDM is designed by using the Lagrangian method; meanwhile, a method using the position and torque sensors mounted on the joints of *iLeg* is designed to indirectly measure the joint angles and torques of the human leg. Then an OET parameterized by the FFS method and optimized by the PSO algorithm is designed and implemented on *iLeg* when the human leg is bound on it. The undetermined parameters of the HLDM are estimated by using the LSE method and the data measured from the OET trajectory. Finally, the dynamic model of the HRI is obtained by combining the dynamic model of *iLeg* and the HLDM, and validated by the experiment. Future work will focus on the application of the dynamic model of the HRI obtained in this paper and further improvement of the performance.

V. Acknowledgments

This research is supported in part by the National Natural Science Foundation of China (Grants 61225017, 61175076 and 61203342), and the International S&T Cooperation Project of China (Grant 2011DFG13390).

References

[1] M. Liu, B. Wu, W.Z. Wang, L.M. Lee, S.H. Zhang, and L.Z. Kong, "Stroke in China: epidemiology, prevention, and management strategies," *The Lancet Neurology*, vol. 6, pp. 456-464, 2007.

[2] X. Li, E.J. Curry, M. Blais, R. Ma, and A.S. Sungarian, "Intraspinal penetrating stab injury to the middle thoracic spinal cord with no neurologic deficit," *Orthopedics*, vol. 35, pp. e770-3, 2012.

[3] M. Lotze, C. Braun, N. Birbaumer, S. Anders, and L.G. Cohen, "Motor learning elicited by voluntary drive," *Brain*, vol. 126, pp. 866-872, 2003.

[4] B. Nan, M. Okamoto, and T. Tsuji, "A hybrid motion classification approach for EMG-based human-robot interfaces using Bayesian and neural networks," *IEEE Transactions on Robotics*, vol. 25, pp. 502-511, 2009.

[5] L.C. Parra, C.D. Spence, A.D. Gerson, and P. Sajda, "Response error correction-a demonstration of improved human-machine performance using real-time EEG monitoring," *IEEE Transactions on Neural Systems and Rehabilitation Engineering*, vol. 11, pp. 173-177, 2003.

[6] J. Musić, R. Kamnik, and M. Munih, "Model based inertial sensing of human body motion kinematics in sit-to-stand movement," *Simulation Modelling Practice and Theory*, vol. 16, pp. 933-944, 2008.

[7] D. Maita and G. Venture, "Influence of the model's degree of freedom on human body dynamics identification," in *Proceedings of the 2013 Annual International Conference of the IEEE in Engineering in Medicine and Biology Society (EMBC)*, Osaka, Japan, Jul. 2013, pp. 4609-4612.

[8] G. Venture, K. Ayusawa, and Y. Nakamura, "Real-time identification and visualization of human segment parameters," in *Proceedings of the 2009 Annual International Conference of the IEEE in Engineering in Medicine and Biology Society (EMBC)*, Minneapolis, USA, Sept. 2009, pp. 3983-3986.

[9] G. Venture and C. Hamon, "Motion recognition from contact forces information and identification of the human body dynamics," in *Proceedings of the 2010 3rd IEEE RAS & EMBS International Conference on Biomedical Robotics and Biomechatronics (BioRob)*, Tokyo, Japan, Sept. 2010, pp. 295-300.

[10] C.C. De Wit, P. Noel, A. Aubin, and B. Brogliato, "Adaptive friction compensation in robot manipulators: Low velocities," *International Journal of Robotics Research*, vol. 10, pp. 189-199, 1991.

[11] J. Swevers, C. Ganseman, D.B. Tukel, J. DeSchutter, and H. VanBrussel, "Optimal robot excitation and identification," *IEEE Transactions on Robotics and Automation*, vol. 13, pp. 730-740, 1997.

[12] M. Gautier and W. Khalil, "Exciting trajectories for the identification of base inertial parameters of robots," *International Journal of Robotics Research*, vol. 11, pp. 362-375, 1992.

[13] J. Kennedy and R. Eberhart, "Particle swarm optimization," in *Proceedings of the 1995 IEEE International Conference on Neural Networks*, Perth, Australia, Nov./Dec. 1995, pp. 1942-1948.

[14] W. Khalil, M. Gautier, and P. Lemoine, "Identification of the payload inertial parameters of industrial manipulators," in *Proceedings of the 2007 IEEE International Conference on Robotics and Automation*, Apr. 2007, pp. 4943-4948.